AGU PUBLICATIONS

Geophysical Research Letters

RESEARCH LETTER
10.1002/2015GL067569

Key Points:
- Low effective normal stress promotes velocity weakening behavior of blueschist faults
- Nucleation of instabilities such as slow earthquakes is promoted by high pore pressure
- Unstable behavior occurs in blueschist under Tohoki-oki hypocentral PT conditions

Supporting Information:
- Supporting Information S1

Correspondence to:
M. Sawai,
msawai@chiba-u.jp

Citation:
Sawai, M., A. R. Niemeijer, O. Plümper, T. Hirose, and C. J. Spiers (2016), Nucleation of frictional instability caused by fluid pressurization in subducted blueschist, *Geophys. Res. Lett.*, *43*, 2543–2551, doi:10.1002/2015GL067569.

Received 23 DEC 2015
Accepted 24 FEB 2016
Published online 24 MAR 2016

Nucleation of frictional instability caused by fluid pressurization in subducted blueschist

Michiyo Sawai[1,2], André R. Niemeijer[3], Oliver Plümper[3], Takehiro Hirose[1,4], and Christopher J. Spiers[3]

[1]Department of Earth and Planetary Systems Science, Graduate School of Science, Hiroshima University, Higashi-Hiroshima, Japan, [2]Now at Department of Earth Sciences, Faculty of Science, Chiba University, Chiba, Japan, [3]Department of Earth Sciences, Utrecht University, Utrecht, Netherlands, [4]Kochi Institute for Core Sample Research, JAMSTEC, Nankoku, Japan

Abstract Pore pressure is an important factor in controlling the slip instability of faults and thus the generation of earthquakes. Particularly slow earthquakes are widespread in subduction zones and usually linked to the occurrence of high pore pressure. Yet the influence of fluid pressure and effective stress on the mechanics of earthquakes is poorly understood. Therefore, we performed shear experiments on blueschist fault rocks, which likely exist at depth in cold and old subduction zones, to investigate the influence of effective stress on frictional behavior. Our results show potentially unstable behavior at temperatures characterizing the seismogenic zone, as well as a transition from stable to unstable behavior with decreasing effective normal stress, which is mechanically equivalent to increasing fluid pressure. This transition is a prerequisite for generating slow earthquakes. Our results imply that high pore pressures are a key factor for nucleating slip leading to both megathrust and slow earthquakes.

1. Introduction

Most large subduction zone earthquakes occur within the subducting oceanic crust. However, such earthquakes are observed in old and cold subducting plates (e.g., northern Japan and Alaska) but not in younger, warm plates (e.g., southwest Japan and Cascadia) [*Abers et al.*, 2013]. This difference in the location of seismicity may be explained by the thermal structures of each subduction zone and the depth range of major metamorphic dehydration reactions [*Hacker et al.*, 2003; *Abers et al.*, 2013]. Pore pressure raised by dehydration is an important control on the strength and instability of faults [e.g., *Davis et al.*, 1983], yet its influence on the mechanics of earthquakes is poorly understood. In cold subduction zones, such as northeast Japan, blueschist dominates the metamorphosed crust. Therefore, understanding the frictional properties of blueschist under various temperature and pressure conditions is crucial in deciphering the nucleation mechanisms of earthquakes in cold subduction zones.

Recent studies suggest that slow earthquakes (e.g., slow-slip events (SSEs), episodic tremor and slip (ETS), and low-frequency earthquakes (LFE)) are linked to regions of high pore pressure [e.g., *Segall et al.*, 2010; *Shibazaki et al.*, 2010; *Sugioka et al.*, 2012]. Similar to normal earthquakes, slow earthquakes release tectonic stresses accumulated along subduction zones, yet they are characterized by much lower moment release rates occurring over periods of minutes to years rather than within several seconds as observed for normal earthquakes [e.g., *Ihmlé and Jordan*, 1994]. Although slow earthquakes often occur outside the conventional seismogenic zone [e.g., *Schwartz and Rokosky*, 2007], recently recorded slow-slip phenomena within seismogenic zones seem to precede large earthquakes, such as the devastating Tohoku megathrust earthquake (M_w of 9.0) [*Kato et al.*, 2012; *Ito et al.*, 2013; *Uchida et al.*, 2016]. Furthermore, low-frequency tremor migration was recorded with an elevated tremor rate for 3 months before the 2004 Parkfield earthquake [*Shelly*, 2009]. Hence, understanding the behavior of slow earthquakes will also allow us to gain a deeper understanding into the generation of megathrust earthquakes.

Consider a simple spring-slider system, in which the slider follows rate-and-state friction (RSF) laws. Linear stability analysis of such a system predicts that an instability can only occur when the friction parameter $(a-b)$ is negative and the stiffness of the slider K is smaller than the critical stiffness K_{cr} that is given by [*Rice and Ruina*, 1983]

$$K < K_{cr} = \frac{-(a-b)\sigma_n^{eff}}{d_c} \quad (1)$$

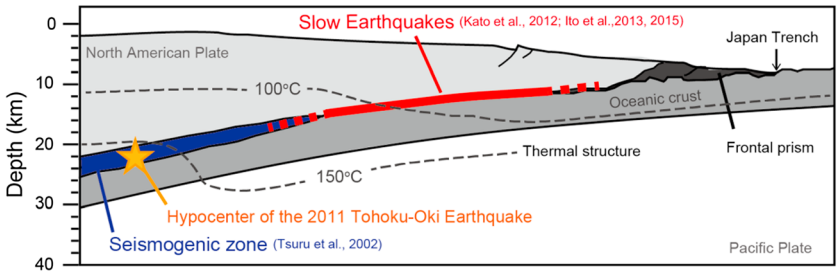

Figure 1. Schematic illustration of the Tohoku subduction zone (modified from *Tsuru et al.* [2000, 2002]). Red line shows the area of slow earthquakes [*Kato et al.*, 2012; *Ito et al.*, 2013, 2015], blue area depicts the seismogenic zone [*Tsuru et al.*, 2002], yellow star indicates the hypocenter of the 2011 Tohoku earthquake, and black dashed lines are the isothermal lines reported from *Kimura et al.* [2012].

where ${\sigma_n}^{\mathrm{eff}}$ is effective normal stress and d_c is critical slip distance. Hence, the stability of the system depends strongly on the two frictional parameters, d_c and $(a-b)$, where $(a-b)$ is defined as the velocity (V) dependence of steady state friction μ_{ss} [*Marone*, 1998; *Scholz*, 1998]:

$$(a-b)=\frac{\partial \mu_{ss}}{\partial \ln V} \tag{2}$$

If $(a-b)\geq 0$, the material exhibits velocity strengthening behavior, which is intrinsically stable. On the other hand, if $(a-b)<0$, the material is velocity weakening and a seismic rupture might be able to nucleate. Furthermore, modeling studies confirmed that small but positive values of K_{cr} are necessary for producing slow-slip events [e.g., *Liu and Rice*, 2007; *Shibazaki and Shimamoto*, 2007]. In the case of constant d_c, the conditions to generate slow earthquakes are attained by either small negative $(a-b)$ or negative $(a-b)$ but low effective stress (i.e., high pore fluid pressure). In addition, different slip styles of slow earthquake (SSEs, LFE, and ETS) can be obtained via models with varying d_c as long as the product of $(a-b)$ and ${\sigma_n}^{\mathrm{eff}}$ is a small negative value [*Shibazaki et al.*, 2010]. It is hence essential to find the variation of $(a-b)$ with pressure and temperature for the material present in a seismogenic zone to constrain the depth range under which both megathrust earthquakes and slow-slip events may nucleate.

The existence of high pore pressure due to fluids released through metamorphic dehydration is expected at the depth range of the occurrence of slow earthquake along various subduction zones [e.g., *Kodaira et al.*, 2004; *Shelly et al.*, 2006]. According to the dense, continuous seismic observations of the 2011 Tohoku earthquake, the main shock was preceded by SSEs and ETS that were located in the rupture area during the earthquake [*Kato et al.*, 2012; *Ito et al.*, 2013, 2015] (Figure 1). The series of the events was also considered to be related to high pore pressure along the Tohoku plate boundary [*Ito et al.*, 2013]. To investigate the influence of elevated fluid pressure, thought to be responsible for both megathrust and slow earthquakes, we conducted friction experiments on powdered samples of blueschist rocks under pressure and temperature conditions similar to those found within cold subduction zones. We particularly investigate the effect of effective normal stress (normal stress minus fluid pressure) on the parameter $(a-b)$ to elucidate how this may affect the potential to trigger megathrust and slow earthquakes.

2. Material and Methods

In this study, we chose lawsonite blueschist as the representative material at seismogenic zones along cold and old subduction zones (e.g., on the basis of the location of the Tohoku earthquake hypocenter and considerations of mineral phases (Figure S1 in the supporting information)). The main components of the rock are glaucophane and lawsonite (Figure S2). It is crucial to investigate frictional properties of rocks present at cold subducted slab, such as the Tohoku plate boundary, in order to constrain modeling analyses and explore the nucleation mechanisms of earthquakes. The blueschist blocks were collected from the Franciscan Belt, Tiburon Peninsula, Marin County, California, which is compatible with the range in conditions of $170<T<220$°C and $3<P<8$ kbar [*Cloos*, 1982]. X-ray diffraction (XRD) analysis and thin section observation revealed that the blueschist consists of glaucophane and lawsonite with minor amount of

titanite, pyrite, garnet, and chlorite (Figure S2). The blueschist was crushed with pestle and mortar and sieved to obtain a powder with a grain size smaller than 125 μm, which formed the simulated gouges for the experiments.

Friction experiments on simulated blueschist gouge were conducted using the hydrothermal ring shear apparatus at Utrecht University (described in detail by *Niemeijer et al*. [2008] and *den Hartog et al*. [2012b]) (Figure S3). Simulated gouges with an initial thickness between 0.6 and 1.0 mm were located between two roughened opposing Ni-superalloy (René 41) pistons. The gouge sample was kept in place by inner and outer confining René 41 rings with diameters of 22 and 28 mm, respectively. The confining rings were coated with Molykote spray to reduce wall friction and dried at 150°C to remove volatiles before assembly. The piston-sample assembly was then loaded inside an internally heated pressure vessel filled with distilled water. Normal stress was first applied, and then pore fluid pressure was increased gradually. After that, a furnace was heated to a desired temperature while keeping the fluid pressure constant. The system was subsequently left to equilibrate under desired temperature and pressure conditions for about 1 h after which shear of the gouge was started using a servo-controlled electromotor, connected via two 1:100 reduction gear boxes. Experiments were performed at temperatures (T) of 22–400°C, effective normal stresses (σ_n^{eff}) of 25–200 MPa and pore fluid pressures (P_f) of 25–200 MPa, which includes the pressure and temperature conditions of the seismogenic zone in cold subduction zones. We set the effective normal stress equal to the pore fluid pressure so that the pore fluid factor λ was fixed ($\lambda = P_f/\sigma_n = 0.5$) in all experiments. In a run, effective stress increased stepwise from 25 to 200 MPa. At each effective normal stress step, velocity stepping tests between 0.1 and 100 μm/s were conducted to determine the friction rate parameter ($a - b$) and critical slip distance (d_c) using standard techniques [*Marone*, 1998]. In general, slip velocity of aseismic slip events, estimated from the average slip and duration of event, range from 10^{-9} to 10^{-7} m/s [e.g., *Dragert et al*., 2001; *Hirose and Obara*, 2005; *Ohta et al*., 2006].

The velocity dependence of friction was interpreted using the Dieterich type evolution RSF equation [*Dieterich*, 1978, 1979; *Ruina*, 1983].

$$\mu = \mu_0 + a\ln\left(\frac{V}{V_0}\right) + b\ln\left(\frac{V_0\theta}{d_c}\right), \quad \text{with} \quad \frac{d\theta}{dt} = 1 - \frac{V\theta}{d_c} \tag{3}$$

where μ_0 is a reference friction coefficient at a reference velocity V_0 and μ is a instantaneous friction coefficient at an instantaneous velocity V. θ is a state variable describing the transient frictional behavior between steady state. To obtain the a, b, and d_c, we used the inversion technique described by *Saffer and Marone* [2003]. The constitutive parameters were determined using the XLook program developed at Pennsylvania State University. Microstructural investigations of deformed samples were carried out using a JEOL JSM-6000 scanning electron microscope equipped with an energy-dispersive X-ray detector.

3. Results

The apparent friction coefficient (shear stress divided by effective normal stress, ignoring cohesion) ranges between 0.7 and 0.9 at temperatures of 22–200°C but lowers to about 0.5–0.6 at 300 and 400°C (Figure 2a). Stick-slip behavior is found only at 200 and 300°C. There are considerable displacement hardening and weakening episodes above 300°C. These might be due to partial dehydration of lawsonite, which contains approximately 11.5 wt % water in its crystal structure and which is stable at temperatures of 150 to 400°C and pressures of 0.3 to 1.0 GPa [*Pawley*, 1994]. This likely reacts to form denser hydrous zeolite or prehnite phases during the dehydration reaction at pressures < 300 MPa and temperature <350°C [*Deer et al*., 1966], although we could not confirm the presence of such reaction products by either thin-section observations or XRD analyses on material recovered after the experiments. The parameter ($a - b$) varies with increasing temperature. It decreases from being positive at <100°C to negative values at 200°C, while it returns to near zero or positive at a temperature of 300°C for any effective normal stress condition and decreases again at 400°C (Figures 2b and S4). Velocity weakening behavior promoted at high temperature again is caused by an increase in the parameter b (Figures 3a, 3f, and S4). The velocity stepping tests yield a d_c of 0.05 to 0.7 mm (Figure S4), which are consistent with typical values of other major rock types measured in rotary shear experiments [e.g., *den Hartog et al*., 2012a]. Contrary to ($a - b$), d_c does not vary systematically with temperature or effective normal stress across the investigated experimental range.

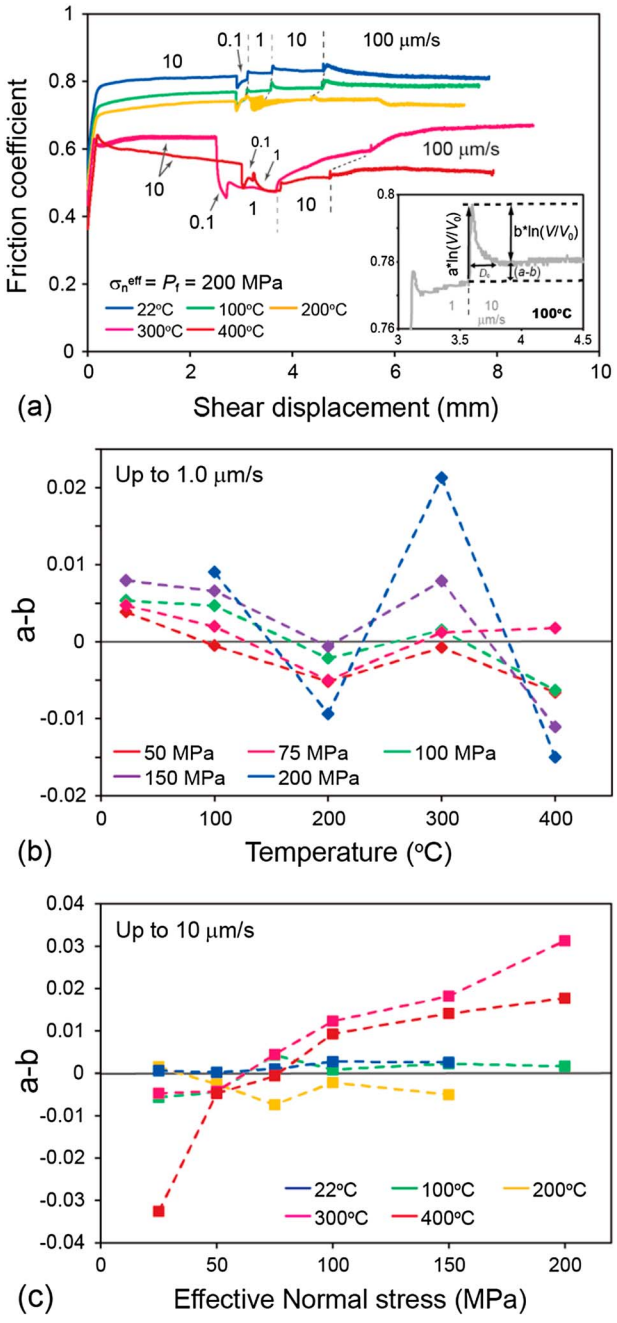

Figure 2. Representative frictional behavior of blueschist powder. (a) Friction coefficient versus displacement curves in velocity stepping tests between 0.1 and 100 μm/s under an effective normal stress of 200 MPa with different temperatures. Inserted plot shows the procedure used to quantify the velocity-dependent behavior in terms of $(a-b)$, for experiment conducted at 100°C. (b) $(a-b)$ at postslip velocity of 1.0 μm/s plotted against temperature with different effective stresses. (c) $(a-b)$ at postslip velocity of 10 μm/s plotted against effective normal stress (σ_n^{eff}) at different temperature conditions.

The effect of effective normal stress on the parameter $(a-b)$ at postslip velocity of 10 μm/s is shown in Figure 2c as a representative step. At any temperature except at 200°C, $(a-b)$ tends to decrease from positive to negative values with decreasing effective normal stress, and it exhibits almost neutral values at an effective normal stress of 50 MPa (Figures 2c and S5). However, neutral to negative $(a-b)$ values are observed at a temperature of 200°C over the entire effective normal stress range tested (25–200 MPa). Furthermore, the velocity weakening behavior is apparent at postslip velocity of 1 μm under the conditions of 400°C and effective normal stresses of 100–200 MPa, although velocity strengthening behavior occurs at higher slip rates. The decreasing trend in $(a-b)$ values with decreasing effective normal stress is caused by an increase in the parameter b (Figures 3 and S5). Thus, the rate parameter $(a-b)$ is significantly dependent on effective normal stress at all temperatures investigated, except 200°C. Our experimental findings imply that a lower effective normal stress promotes negative values of $(a-b)$ and thus the potential to nucleate a frictional instability.

4. Discussion and Conclusion

He et al. [2007] conducted friction experiments on gabbro gouge at effective normal stresses of 200 and 300 MPa at temperatures of 21–615°C. They reported that negative $(a-b)$ values appeared only at the lowest effective normal stress condition and at temperatures ranging from 170 to 310°C and thus concluded that a lower effective normal stress condition is favorable for velocity weakening behavior. Such a transition from velocity strengthening to weakening with decreasing normal stress has also been reported for smectite gouge during room temperature experiments [*Saffer and Marone*, 2003]. Together with our results, we infer that the effective normal stress is a significant factor controlling the rate parameter $(a-b)$ and thus slip stability, although the effective normal stress conditions necessary for the transition from velocity strengthening to weakening seem to vary depending on rock type, slip velocity, and temperature. The broader implication of our results is that friction parameters for earthquake modeling should be determined on the actual materials expected to be present

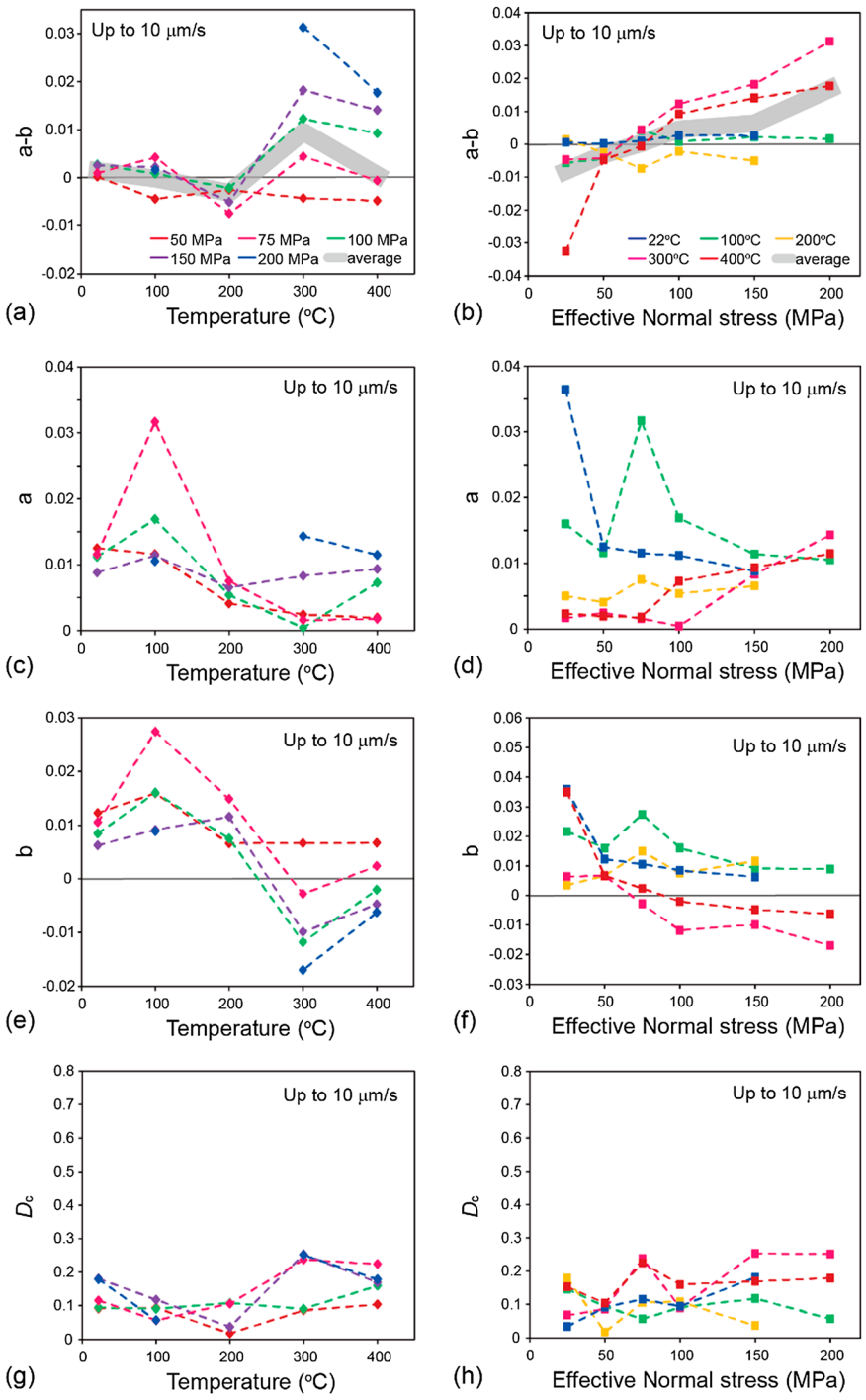

Figure 3. Representative rate-and-state friction parameters plotted against (a, c, e, and g) temperature and (b, d, f, and h) effective normal stress. All data are the results at postslip velocity of 10 μm/s. Gray line in Figures 3a and 3b shows the mean data values for each temperature or pressure conditions.

along the plate boundary interface, at realistic (preferably in situ) P-T-stress conditions and shearing rate (from approximately nm/s to approximately mm/s for slow earthquakes).

As mentioned in section 1, whether an instability can occur or not, in the framework of rate-and-state friction, depends on the relative magnitudes of the stiffness K of the slider and of the critical stiffness K_{cr} (equation (1)). Stable slip occurs without an earthquake when $K_{cr} < 0$ (i.e. $(a - b) > 0$), but slip is unstable when $K < K_{cr}$. Slip is conditionally stable, which includes the potential for slow earthquakes, when $0 < K_{cr} < K$ with $(a - b) < 0$. We

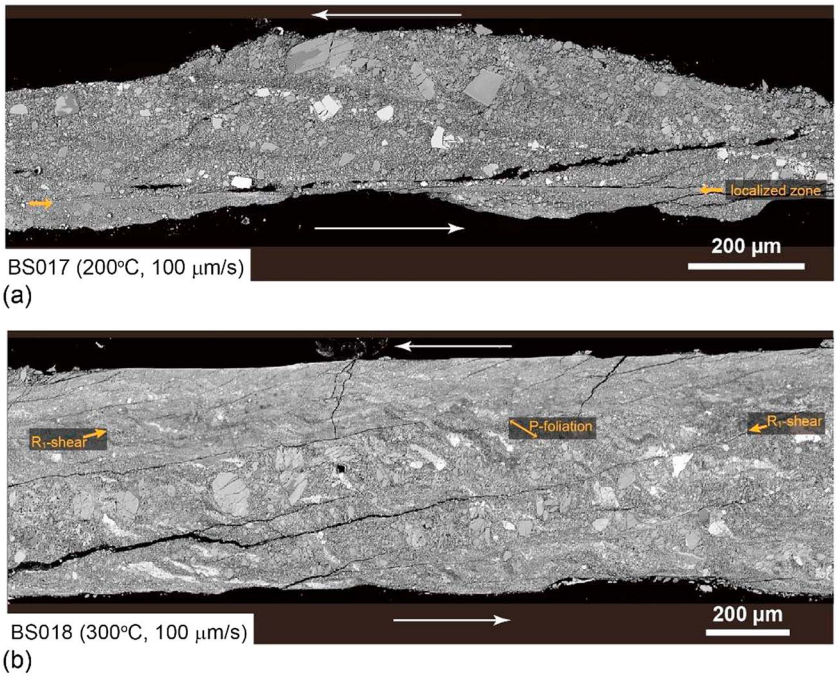

Figure 4. Backscattered electron images of the experimental samples acquired in a scanning electron microscope. (a) The blueschist sample after 15 mm displacement at $T = 200$°C, $V = 100$ μm/s, and $\sigma_n^{eff} = P_f = 75$ MPa. At this condition where the sample shows velocity weakening behavior, a sharp, highly localized shear zone is observed in the fault zone (yellow arrows). (b) The blueschist sample deformed at $T = 300$°C, $\sigma_n^{eff} = P_f = 75$ MPa, and $V = 100$ μm/s. Frictional behavior is characterized by velocity strengthening at this condition. Deformation is widely dispersed throughout the fault zone with characteristic elongated features of pyrite, lawsonite, and titanite grains. R_1 shear and P foliations are developed in the velocity strengthening one (yellow arrows).

therefore calculated both the stability parameter $(a-b)\sigma_n^{eff}$ and K_{cr} from our data (Figures S6 and S7). The trend exhibited by $(a-b)$ versus σ_n^{eff} is similar to that shown by $(a-b)$, with the transition between positive and negative $(a-b)\sigma_n^{eff}$ values occurring at around 50–75 MPa at all temperatures investigated. The trend in K_{cr} with temperature is less clear than that shown by $(a-b)\sigma_n^{eff}$ (Figure S6), due to the large variability seen in d_c. As a result, the combined effect of temperature and effective normal stress on K_{cr} is not clear-cut, making it difficult to distinguish whether a slow or normal earthquake should be expected. Nonetheless, our results do suggest that effective pressure strongly affects at least the rate-and-state parameter $(a-b)$.

An important question remaining is why low effective stress promotes velocity weakening. In this study, samples deformed under conditions where slip is characterized by velocity weakening always show a clear, localized boundary shear of highly comminuted material whereas velocity strengthening samples do not (Figure 4). A similar correlation between the mechanical behavior and the deformation microstructure has been observed in other experiments [e.g., *Beeler et al*., 1996]. This might be a reason why $(a-b)$ tends to be negative at lower effective stress, although we could not confirm this from the microstructures recovered after effective normal stress stepping at low effective stress.

The changes in $(a-b)$ with temperature and effective normal stress that we observe can alternatively be explained using the microphysical model proposed by *Niemeijer and Spiers* [2007; see also *Den Hartog and Spiers*, 2013; *Den Hartog and Spiers*, 2014]. From the model, decreasing effective normal stress should yield a decrease of $(a-b)$ at any temperature due to a decrease in the relative importance of thermally activated compaction creep process, versus dilatation associated with granular flow. This is because compaction creep is slower at low normal stresses, so steady state porosity will be higher. This in turn implies that the dilatation angle due to granular flow is lower, the steady state frictional strength is lower, and the rate parameter b is higher, so that $(a-b)$ becomes lower. Our results indeed seem to show that b increases with decreasing effective normal stress (Figures 3 and S5). In the two temperature regimes of velocity weakening that we observe, b shows different behavior, being almost constant in the range 22°C to 200°C but increasing with increasing temperature from 300°C to 400°C. Although the microphysical model was developed for mixed gouges containing phyllosilicates, the general concept of a competition

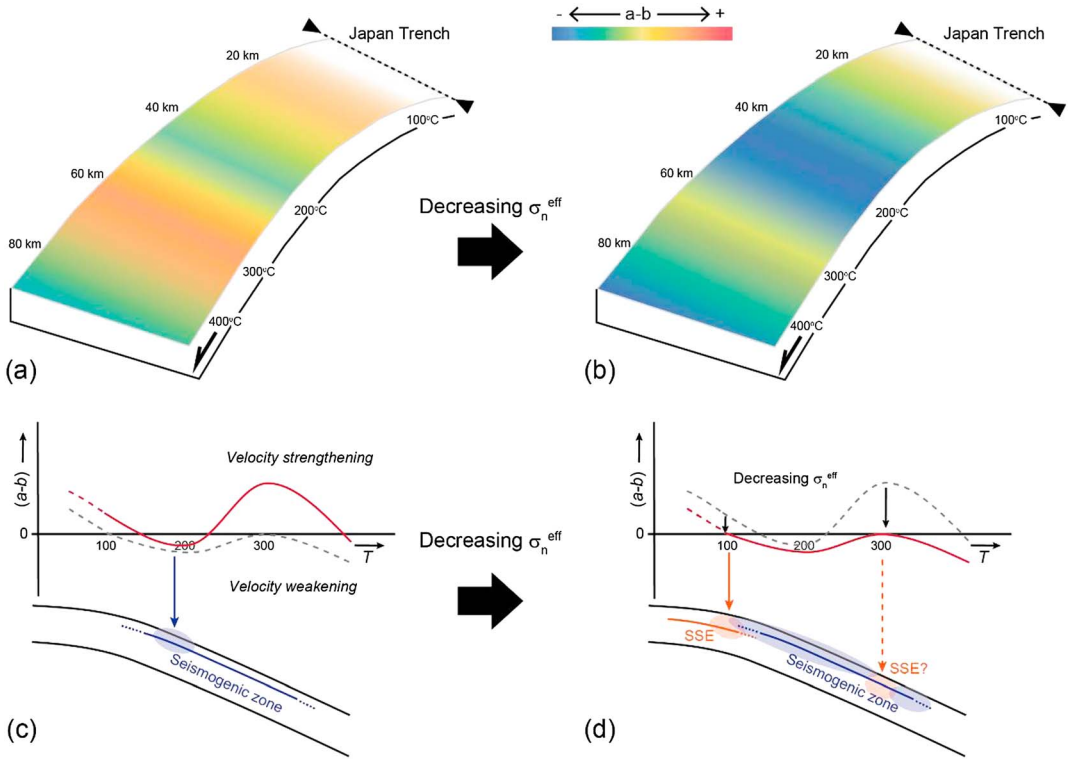

Figure 5. A schematic illustration of the evolution of frictional properties from (a and c) high effective stress (based on the results of σ_n^{eff} = 150 MPa) to (b and d) low effective stress (based on the results of σ_n^{eff} = 50 MPa) (e.g., by increasing fluid pressure) at the Tohoku subduction zone. Figures 5a and 5b are top views of the plate interface. The depth scale is assumed from the geothermal gradients reported at *Peacock and Wang* [1999] (Figure S1). Negative to positive ($a - b$) values are indicated as color gradients from blue to red, respectively. Figures 5c and 5d are cross sections of the subduction zone plotted with possible ($a - b$) versus temperature curves based on the experiments. Note in Figures 5c and 5d that as effective stress decreases, the ($a - b$) curve meets unstable slip conditions over a wide range of temperature (blue circles) and also meets the transition from stable to unstable slip conditions that are necessary to generate slow earthquakes at temperatures of 100 and 300°C (orange circles).

between dilatation and compaction seems suitable to explain our results of changes in the rate-and-state parameters as function of effective normal stress, temperature, and velocity. We speculate that the two temperature regimes of velocity weakening may be caused by different creep mechanisms dominating compaction at higher versus lower temperatures, or/and by the same compaction mechanism dominating at different temperatures in the two main mineral components (glaucophane and lawsonite). Clearly, more work is needed to fully understand the effects of effective normal stress, fluid pressure, and temperature on a, b and ($a - b$).

Our results have important implications for the generation of diverse slip styles in cold and old subduction zones. First, despite the broad range of effective normal stress range studied, the blueschist that is likely present at seismogenic depths in the subducted slab exhibited velocity weakening behavior *only* at ~200°C (Figure 2). Considering the Tohoku subduction area as a representative cold and old subduction zone, since the temperature at the hypocenter of the 2011 Tohoku earthquake is estimated to be 150–200°C (Figure 1), this frictional property could be consistent with the initiation of the Tohoku earthquake. Second, at temperatures lower than ~150°C or higher than 250°C, the transition from velocity strengthening to weakening occurs when effective normal stress is lower (e.g., due to an increase in pore fluid pressure) (Figure 2). A transition that leads to the rate parameter ($a - b$) being negative but close to zero meets the conditions necessary for the generation of slow earthquakes [*Shibazaki et al.*, 2010]. Our results therefore imply that slow earthquakes could be caused by elevated fluid pressure that progressively lowers the value of ($a - b$) along the Tohoku plate boundary during an interseismic period, promoting the nucleation of earthquakes (Figure 5).

Our current model, based on the dependence of the frictional properties of blueschist upon fluid pressure can account for the generation of the Tohoku megathrust earthquake as well as that of slow

earthquakes (Figure 5). However, to date, there have been no observations of slow earthquakes in the deep portions of the Tohoku plate boundary, which we would expect from our model as well as from seismic observations from other subduction zones such as Nankai trough [*Obara*, 2002]. Further studies including friction experiments under realistic seismogenic conditions, as well as numerical simulations [e.g., *Noda and Lapusta*, 2013] that incorporate the effect of evolving fluid pressure on fault constitutive parameters, are required to solve this discrepancy and to unravel the relationship between slow earthquakes and megathrust earthquakes.

Acknowledgments

We would like to express our sincere thanks to Matt Ikari, an anonymous reviewer, and the Associate Editor Ake Fagereng for careful and constructive review which improved our paper. We appreciate the advice of S.A.M. den Hartog and Colin Peach when using the Utrecht ring shear instrument, and the first author expresses special thanks to S.A.M. den Hartog for her instruction in using the apparatus. We also thank to Peter van Krieken (Utrecht University) and Osamu Tadai (Kochi Institute for Core Sample Research, JAMSTEC) for their help in conducting XRD analyses. Technical support in maintaining the ring shear machine was provided by T. van der Gon Netscher, G. Kastelein, and E. de Graaff. This study was supported by a grant-in-aid for JSPS Fellows (to M. Sawai), a Grant-in-Aid for Young Scientists (start-up) 15H06890 (to M. Sawai) and JSPS KAKENHI grant 25287135 (to T. Hirose). A. Niemeijer is supported by the Netherlands Organisation for Scientific Research (NWO) through a VIDI grant (854.12.011) and by the ERC starting grant SEISMIC (335915). O. Plümper is supported by a NWO Veni grant (863.13.006).

References

Abers, G. A., J. Nakajima, P. E. van Keken, S. Kita, and B. R. Hacker (2013), Thermal-petrological controls on the location of earthquakes within subducting plates, *Earth Planet. Sci. Lett.*, *369-370*, 178–187, doi:10.1016/j.epsl.2013.03.022.

Beeler, N. M., T. E. Tullis, M. L. Blanpied, and J. D. Weeks (1996), Frictional behavior of large displacement experimental faults, *J. Geophys. Res.*, *101*, 8697–8715.

Cloos, M. (1982), Flow melanges: Numerical modeling and geologic constraints on their origin in the Franciscan subduction complex, California, *Geol. Soc. Am. Bull.*, *93*(4), 330–345.

Davis, D. M., J. Suppe, and F. A. Dahlen (1983), The mechanics of fold-and-thrust belts, *J. Geophys. Res.*, *88*(B2), 1153–1172, doi:10.1029/JB088iB02p01153.

Deer, W. A., R. A. Howie, and J. Zussman (1966), Rock-forming minerals [Russian translation], *Mir*, *Moscow*, *4*.

Den Hartog, S. A. M., and C. J. Spiers (2013), Influence of subduction zone conditions and gouge composition on frictional slip stability of megathrust faults, *Tectonophysics*, *600*, 75–90, doi:10.1016/j.tecto.2012.11.006.

Den Hartog, S. A. M., and C. J. Spiers (2014), A microphysical model for fault gouge friction applied to subduction megathrusts, *J. Geophys. Res. Solid Earth*, *119*, 1510–1529, doi:10.1002/2013JB010580.

Den Hartog, S. A. M., A. R. Niemeijer, and C. J. Spiers (2012a), New constraints on megathrust slip stability under subduction zone P-T conditions, *Earth Planet. Sci. Lett.*, *353-354*, 240–252, doi:10.1016/j.epsl.2012.08.022.

Den Hartog, S. A. M., C. J. Peach, D. A. M. De Winter, C. J. Spiers, and T. Shimamoto (2012b), Frictional properties of megathrust fault gouges at low sliding velocities: New data on effects of normal stress and temperature, *J. Struct. Geol.*, *38*, 156–171, doi:10.1016/j.jsg.2011.12.001.

Dieterich, J. H. (1978), Time-dependent friction and the mechanics of stick-slip, *Pure Appl. Geophys.*, *116*, 790–806.

Dieterich, J. H. (1979), Modeling of rock friction: 1. Experimental results and constitutive equations, *J. Geophys. Res.*, *84*(B5), 2161–2168.

Dragert, H., K. Wang, and T. S. James (2001), A silent slip event on the deeper Cascadia subduction interface, *Science*, *292*, 1525–1528, doi:10.1126/science.1060152.

Hacker, B. R., S. M. Peacock, G. A. Abers, and S. D. Holloway (2003), Subduction factory: 2. Are intermediate-depth earthquakes in subducting slabs linked to metamorphic dehydration reactions? *J. Geophys. Res.*, *108*(B1), 2030, doi:10.1029/2001JB001129.

He, C., Z. Wang, and W. Yao (2007), Frictional sliding of gabbro gouge under hydrothermal conditions, *Tectonophysics*, *445*, 353–362, doi:10.1016/j.tecto.2007.09.008.

Hirose, H., and K. Obara (2005), Repeating short- and long-term slow slip events with deep tremor activity around the Bungo channel region, southwest Japan, *Earth Planet. Space*, *57*, 961–972.

Ihmlé, P. F., and T. H. Jordan (1994), Teleseismic search for slow precursors to large earthquakes, *Science*, *266*, 1547–1551, doi:10.1126/science.266.5190.1547.

Ito, Y., et al. (2013), Episodic slow slip events in the Japan subduction zone before the 2011 Tohoku-Oki earthquake, *Tectonophysics*, *600*, 14–26, doi:10.1016/j.tecto.2012.08.022.

Ito, Y., R. Hino, S. Suzuki, and Y. Kaneda (2015), Episodic tremor and slip near the Japan Trench prior to the 2011 Tohoku-Oki earthquake, *Geophys. Res. Lett.*, *42*, 1725–1731, doi:10.1002/2014GL062986.

Kato, A., K. Obara, T. Igarashi, H. Tsuruoka, S. Nakagawa, and N. Hirata (2012), Propagation of slow slip leading up to the 2011 M_W 9.0 Tohoku-Oki earthquake, *Science*, *335*, 705–708, doi:10.1126/science.1215141.

Kimura, G., S. Hina, Y. Hamada, J. Kameda, T. Tsuji, M. Kinoshita, and A. Yamaguchi (2012), Runaway slip to the trench due to rupture of highly pressurized megathrust beneath the middle trench slope: The tsunamigenesis of the 2011 Tohoku earthquake off the east coast of northern Japan, *Earth Planet. Sci. Lett.*, *339-340*, 32–45, doi:10.1016/j.epsl.2012.04.002.

Kodaira, S., T. Iidaka, A. Kato, J. O. Park, T. Iwasaki, and Y. Kaneda (2004), High pore fluid pressure may cause silent slip in the Nankai Trough, *Science*, *304*(5675), 1295–1298, doi:10.1126/science.1096535.

Liu, Y., and J. R. Rice (2007), Spontaneous and triggered aseismic deformation transients in a subduction fault model, *J. Geophys. Res.*, *112*, B09404, doi:10.1029/2007JB004930.

Marone, C. (1998), Laboratory-derived friction laws and their application to seismic faulting, *Annu. Rev. Earth Planet. Sci.*, *26*, 643–696, doi:10.1146/annurev.earth.26.1.643.

Niemeijer, A. R., and C. J. Spiers (2007), A microphysical model for strong velocity weakening in phyllosilicate-bearing fault gouges, *J. Geophys. Res.*, *112*, B10405, doi:10.1029/2007JB005008.

Niemeijer, A. R., C. J. Spiers, and C. J. Peach (2008), Frictional behaviour of simulated quartz fault gouges under hydrothermal conditions: Results from ultra-high strain rotary shear experiments, *Tectonophysics*, *460*, 288–303, doi:10.1016/j.tecto.2008.09.003.

Noda, H., and N. Lapusta (2013), Stable creeping fault segments can become destructive as a result of dynamic weakening, *Nature*, *493*, 518–521.

Obara, K. (2002), Non-volcanic deep tremor associated with subduction in southwest Japan, *Science*, *296*, 1679–1681, doi:10.1126/science.1070378.

Ohta, Y., J. T. Freymuller, S. Hreinsdóttir, and H. Suito (2006), A large slow slip event and the depth of the seismogenic zone in the south central Alaska subduction zone, *Earth Planet. Sci. Lett.*, *247*, 108–116.

Pawley, A. R. (1994), The pressure and temperature stability limits of lawsonite: Implications for H_2O recycling in subduction zones, *Cont. Min. Pet.*, *118*(1), 99–108.

Peacock, S. M., and K. Wang (1999), Seismic consequences of warm versus cool subduction metamorphism: Examples from southwest and northeast Japan, *Science*, *286*, 937–939, doi:10.1126/science.286.5441.937.

Rice, J. R., and A. L. Ruina (1983), Stability of steady frictional slipping, *J. Appl. Mech.*, *50*(2), 343–349.

Ruina, A. (1983), Slip instability and state variable friction laws, *J. Geophys. Res.*, *88*(B12), 10,359–10,370.
Saffer, D. M., and C. Marone (2003), Comparison of smectite- and illite-rich gouge frictional properties: Application to the updip limit of the seismogenic zone along subduction megathrusts, *Earth Planet. Sci. Lett.*, *215*(1-2), 219–235, doi:10.1016/S0012-821X(03)00424-2.
Scholz, C. H. (1998), Earthquakes and friction laws, *Nature*, *391*, 37–42, doi:10.1038/34097.
Schwartz, S. Y., and J. M. Rokosky (2007), Slow slip events and seismic tremor at circum-Pacific subduction zones, *Rev. Geophys.*, *45*, RG3004, doi:10.1029/2006RG000208.
Segall, P., A. M. Rubin, A. M. Bradley, and J. R. Rice (2010), Dilatant strengthening as a mechanism for slow slip events, *J. Geophys. Res.*, *115*, B12305, doi:10.1029/2010JB007449.
Shelly, D. R. (2009), Possible deep fault slip preceding the 2004 Parkfield earthquake, inferred from detailed observations of tectonic tremor, *Geophys. Res. Lett.*, *36*, L17318, doi:10.1029/2009GL039589.
Shelly, D. R., G. C. Beroza, S. Ide, and S. Nakamula (2006), Low-frequency earthquakes in Shikoku, Japan and their relationship to episodic tremor and slip, *Nature*, *442*, 188–191, doi:10.1038/nature04931.
Shibazaki, B., and T. Shimamoto (2007), Modelling of short-interval silent slip events in deeper subduction interfaces considering the frictional properties at the unstable-stable transition regime, *Geophys. J. Int.*, *171*, 191–205, doi:10.1111/j.1365-246X.2007.03434.x.
Shibazaki, B., S. Bu, T. Matsuzawa, and H. Hirose (2010), Modeling the activity of short-term slow slip events along deep subduction interfaces beneath Shikoku, southwest Japan, *J. Geophys. Res.*, *115*, B00A19, doi:10.1029/2008JB006057.
Sugioka, H., T. Okamoto, T. Nakamura, Y. Ishihara, A. Ito, K. Obana, M. Kinoshita, K. Nakahigashi, M. Shinohara, and Y. Fukao (2012), Tsunamigenic potential of the shallow subduction plate boundary inferred from slow seismic slip, *Nat. Geosci.*, *5*, 414–418, doi:10.1038/ngeo1466.
Tsuru, T., J. Park, N. Takahashi, S. Kodaira, Y. Kido, Y. Kaneda, and Y. Kono (2000), Tectonic features of the Japan trench convergent margin off Sanriku, northeastern Japan, revealed by multichannel seismic reflection data, *J. Geophys. Res.*, *105*, 16,403–16,413, doi:10.1029/2000JB900132.
Tsuru, T., J. Park, S. Miura, S. Kodaira, Y. Kido, and T. Hayashi (2002), Along-arc structural variation of the plate boundary at the Japan Trench margin: Implication of interplate coupling, *J. Geophys. Res.*, *107*(B12), 2357, doi:10.1029/2001JB001664.
Uchida, N., T. Iinuma, R. M. Nadeau, R. Bürgmann, and R. Hino (2016), Periodic slow slip triggers megathrust zone earthquakes in northeastern Japan, *Science*, *351*(6272), 488–492.